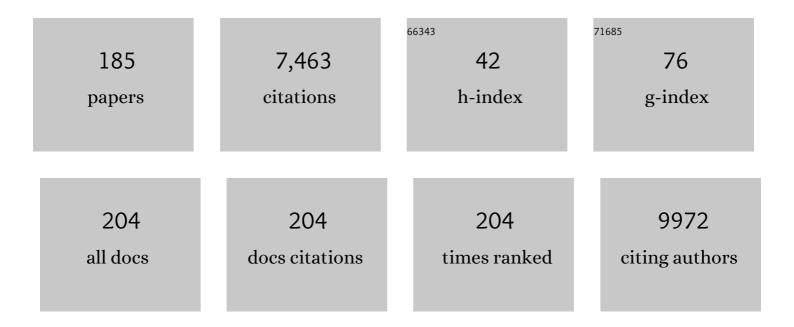
List of Publications by Year in descending order

Source: https://exaly.com/author-pdf/5802761/publications.pdf Version: 2024-02-01



#	Article	IF	CITATIONS
1	Clinical Proton MR Spectroscopy in Central Nervous System Disorders. Radiology, 2014, 270, 658-679.	7.3	524
2	Ventricular enlargement as a possible measure of Alzheimer's disease progression validated using the Alzheimer's disease neuroimaging initiative database. Brain, 2008, 131, 2443-2454.	7.6	393
3	Glutamate and Glutamine Measured With 4.0 T Proton MRS in Never-Treated Patients With Schizophrenia and Healthy Volunteers. American Journal of Psychiatry, 2002, 159, 1944-1946.	7.2	386
4	Methodological consensus on clinical proton MRS of the brain: Review and recommendations. Magnetic Resonance in Medicine, 2019, 82, 527-550.	3.0	280
5	Association of Dual-Task Gait With Incident Dementia in Mild Cognitive Impairment. JAMA Neurology, 2017, 74, 857.	9.0	263
6	Resting state defaultâ€mode network connectivity in early depression using a seed regionâ€ofâ€interest analysis: Decreased connectivity with caudate nucleus. Psychiatry and Clinical Neurosciences, 2009, 63, 754-761.	1.8	260
7	Measurement of Glutamate and Glutamine in the Medial Prefrontal Cortex of Never-Treated Schizophrenic Patients and Healthy Controls by Proton Magnetic Resonance Spectroscopy. Archives of General Psychiatry, 1997, 54, 959.	12.3	217
8	A Short Echo ¹ H Spectroscopy and Volumetric MRI Study of the Corpus Striatum in Patients With Obsessive- Compulsive Disorder and Comparison Subjects. American Journal of Psychiatry, 1998, 155, 1584-1591.	7.2	156
9	Blood pressure levels and brain volume reduction. Journal of Hypertension, 2013, 31, 1502-1516.	0.5	143
10	Reduced hippocampal glutamate in Alzheimer disease. Neurobiology of Aging, 2011, 32, 802-810.	3.1	137
11	Quantitative Tissue Ph Measurement during Cerebral Ischemia Using Amine and Amide Concentration-Independent Detection (AACID) with MRI. Journal of Cerebral Blood Flow and Metabolism, 2014, 34, 690-698.	4.3	137
12	Comparison of the quantification precision of human short echo time1H spectroscopy at 1.5 and 4.0 Tesla. Magnetic Resonance in Medicine, 2000, 44, 185-192.	3.0	128
13	Factors affecting the quantification of short echoin-vivo1H MR spectra: prior knowledge, peak elimination, and filtering. , 1999, 12, 205-216.		117
14	In vivo1H2OT?2 measurement in the human occipital lobe at 4T and 7T by Carr-Purcell MRI: Detection of microscopic susceptibility contrast. Magnetic Resonance in Medicine, 2002, 47, 742-750.	3.0	109
15	A sensitive PARACEST contrast agent for temperature MRI: Eu ³⁺ â€DOTAMâ€glycine (Cly)â€phenylalanine (Phe). Magnetic Resonance in Medicine, 2008, 59, 374-381.	3.0	106
16	Fourâ€pool modeling of proton exchange processes in biological systems in the presence of MRI–paramagnetic chemical exchange saturation transfer (PARACEST) agents. Magnetic Resonance in Medicine, 2008, 60, 1197-1206.	3.0	106
17	The Canadian Dementia Imaging Protocol: Harmonizing National Cohorts. Journal of Magnetic Resonance Imaging, 2019, 49, 456-465.	3.4	101
18	Advanced single voxel ¹ H magnetic resonance spectroscopy techniques in humans: Experts' consensus recommendations. NMR in Biomedicine, 2021, 34, e4236.	2.8	98

#	Article	IF	CITATIONS
19	Functional MRI of pain application in youth who engaged in repetitive non-suicidal self-injury vs. psychiatric controls. Psychiatry Research - Neuroimaging, 2014, 223, 104-112.	1.8	91
20	Motor cortex and gait in mild cognitive impairment: a magnetic resonance spectroscopy and volumetric imaging study. Brain, 2013, 136, 859-871.	7.6	86
21	Stressâ€inducible phosphoprotein 1 has unique cochaperone activity during development and regulates cellular response to ischemia <i>via</i> the prion protein. FASEB Journal, 2013, 27, 3594-3607.	0.5	86
22	Multiparametric MRI changes persist beyond recovery in concussed adolescent hockey players. Neurology, 2017, 89, 2157-2166.	1.1	83
23	Elimination of the Vesicular Acetylcholine Transporter in the Striatum Reveals Regulation of Behaviour by Cholinergic-Glutamatergic Co-Transmission. PLoS Biology, 2011, 9, e1001194.	5.6	80
24	Quantitative proton short-echo-time LASER spectroscopy of normal human white matter and hippocampus at 4 Tesla incorporating macromolecule subtraction. Magnetic Resonance in Medicine, 2003, 49, 918-927.	3.0	79
25	Spectroscopic lineshape correction by QUECC: Combined QUALITY deconvolution and eddy current correction. Magnetic Resonance in Medicine, 2000, 44, 641-645.	3.0	76
26	Aerobic Glycolysis in the Frontal Cortex Correlates with Memory Performance in Wild-Type Mice But Not the APP/PS1 Mouse Model of Cerebral Amyloidosis. Journal of Neuroscience, 2016, 36, 1871-1878.	3.6	75
27	The Ontario Neurodegenerative Disease Research Initiative (ONDRI). Canadian Journal of Neurological Sciences, 2017, 44, 196-202.	0.5	72
28	A short echo proton magnetic resonance spectroscopy study of the left mesial-temporal lobe in first-onset schizophrenic patients. Biological Psychiatry, 1999, 45, 1403-1411.	1.3	69
29	Simultaneous in vivo pH and temperature mapping using a PARACESTâ€MRI contrast agent. Magnetic Resonance in Medicine, 2013, 70, 1016-1025.	3.0	66
30	Vitamin <scp>D</scp> concentration and lateral cerebral ventricle volume in older adults. Molecular Nutrition and Food Research, 2013, 57, 267-276.	3.3	63
31	Brain reorganization in patients with spinal cord compression evaluated using fMRI. Neurology, 2010, 74, 1048-1054.	1.1	59
32	Glutamate and Dysconnection in the Salience Network: Neurochemical, Effective Connectivity, and Computational Evidence in Schizophrenia. Biological Psychiatry, 2020, 88, 273-281.	1.3	58
33	Forebrain Deletion of the Vesicular Acetylcholine Transporter Results in Deficits in Executive Function, Metabolic, and RNA Splicing Abnormalities in the Prefrontal Cortex. Journal of Neuroscience, 2013, 33, 14908-14920.	3.6	56
34	Motor Phenotype in Neurodegenerative Disorders: Gait and Balance Platform Study Design Protocol for the Ontario Neurodegenerative Research Initiative (ONDRI). Journal of Alzheimer's Disease, 2017, 59, 707-721.	2.6	54
35	Combination of memantine and vitamin D prevents axon degeneration induced by amyloid-beta and glutamate. Neurobiology of Aging, 2014, 35, 331-335.	3.1	53
36	Increased glutamate in the hippocampus after galantamine treatment for Alzheimer disease. Progress in Neuro-Psychopharmacology and Biological Psychiatry, 2010, 34, 104-110.	4.8	51

#	Article	IF	CITATIONS
37	Effect of signal-to-noise ratio and spectral linewidth on metabolite quantification at 4 T. NMR in Biomedicine, 2007, 20, 512-521.	2.8	49
38	Vitamin D and brain volumetric changes: Systematic review and meta-analysis. Maturitas, 2014, 78, 30-39.	2.4	49
39	Contribution of Brain Imaging to the Understanding Of Gait Disorders in Alzheimer's Disease. American Journal of Alzheimer's Disease and Other Dementias, 2012, 27, 371-380.	1.9	47
40	Duration of untreated psychosis vs. N-acetylaspartate and choline in first episode schizophrenia: a 1H magnetic resonance spectroscopy study at 4.0 Tesla. Psychiatry Research - Neuroimaging, 2004, 131, 107-114.	1.8	46
41	A Robust and Convergent Synthesis of Dipeptideâ^'DOTAM Conjugates as Chelators for Lanthanide Ions: New PARACEST MRI Agents. Bioconjugate Chemistry, 2007, 18, 1625-1636.	3.6	46
42	Higher Gait Variability is Associated with Decreased Parietal Gray Matter Volume Among Healthy Older Adults. Brain Topography, 2014, 27, 293-295.	1.8	44
43	Comorbid Aβ toxicity and stroke: hippocampal atrophy, pathology, and cognitive deficit. Neurobiology of Aging, 2014, 35, 1605-1614.	3.1	44
44	High field 1H MRS of the hippocampus after donepezil treatment in Alzheimer disease. Progress in Neuro-Psychopharmacology and Biological Psychiatry, 2008, 32, 786-793.	4.8	43
45	A paramagnetic chemical exchange-based MRI probe metabolized by cathepsin D: design, synthesis and cellular uptake studies. Organic and Biomolecular Chemistry, 2010, 8, 2560.	2.8	43
46	Metabolomics profiling of concussion in adolescent male hockey players: a novel diagnostic method. Metabolomics, 2016, 12, 1.	3.0	43
47	MRI and Multinuclear MR Spectroscopy of 3,200-Year-Old Egyptian Mummy Brain. American Journal of Roentgenology, 2007, 189, W105-W110.	2.2	42
48	Proton magnetic resonance spectroscopy of the motor cortex in cervical myelopathy. Brain, 2012, 135, 461-468.	7.6	39
49	Topiramate induces acute intracellular acidification in glioblastoma. Journal of Neuro-Oncology, 2016, 130, 465-472.	2.9	39
50	MouseBytes, an open-access high-throughput pipeline and database for rodent touchscreen-based cognitive assessment. ELife, 2019, 8, .	6.0	38
51	Reduced Hippocampal Glutamate and Posterior Cingulate N-Acetyl Aspartate in Mild Cognitive Impairment and Alzheimer's Disease Is Associated with Episodic Memory Performance and White Matter Integrity in the Cingulum: A Pilot Study. Journal of Alzheimer's Disease, 2020, 73, 1385-1405.	2.6	37
52	Association between gait variability and brain ventricle attributes: a brain mapping study. Experimental Gerontology, 2014, 57, 256-263.	2.8	35
53	Entorhinal Cortex Volume Is Associated With Dual-Task Gait Cost Among Older Adults With MCI: Results From the Gait and Brain Study. Journals of Gerontology - Series A Biological Sciences and Medical Sciences, 2019, 74, 698-704.	3.6	35
54	Semiâ€LASER ¹ H MR spectroscopy at 7 Tesla in human brain: Metabolite quantification incorporating subjectâ€specific macromolecule removal. Magnetic Resonance in Medicine, 2015, 74, 4-12.	3.0	34

#	Article	IF	CITATIONS
55	Low-Grade Glioma: Correlation of Short Echo Time ¹ H-MR Spectroscopy with ²³ Na MR Imaging. American Journal of Neuroradiology, 2008, 29, 464-470.	2.4	33
56	Vitamin D and white matter abnormalities in older adults: A quantitative volumetric analysis of brain MRI. Experimental Gerontology, 2015, 63, 41-47.	2.8	33
57	Anatomic Correlation of the Mini-Mental State Examination: A Voxel-Based Morphometric Study in Older Adults. PLoS ONE, 2016, 11, e0162889.	2.5	33
58	Long component time constant of23NaT*2 relaxation in healthy human brain. Magnetic Resonance in Medicine, 2004, 52, 407-410.	3.0	32
59	Imaging chemical exchange saturation transfer (CEST) effects following tumorâ€selective acidification using lonidamine. NMR in Biomedicine, 2015, 28, 566-575.	2.8	32
60	Multisite Comparison of MRI Defacing Software Across Multiple Cohorts. Frontiers in Psychiatry, 2021, 12, 617997.	2.6	32
61	Repetitive mild traumatic brain injury in mice triggers a slowly developing cascade of long-term and persistent behavioral deficits and pathological changes. Acta Neuropathologica Communications, 2021, 9, 60.	5.2	31
62	Linear aspects of transformation from interictal epileptic discharges to BOLD fMRI signals in an an an an an an	4.2	30
63	In vivo detection of MRIâ€PARACEST agents in mouse brain tumors at 9.4 T. Magnetic Resonance in Medicine, 2011, 66, 67-72.	3.0	30
64	Slow gait in MCI is associated with ventricular enlargement: results from the Gait and Brain Study. Journal of Neural Transmission, 2013, 120, 1083-1092.	2.8	30
65	Dichloroacetate induced intracellular acidification in glioblastoma: in vivo detection using AACID-CEST MRI at 9.4ÂTesla. Journal of Neuro-Oncology, 2018, 136, 255-262.	2.9	30
66	Advances in High-Field Magnetic Resonance Spectroscopy in Alzheimer's Disease. Current Alzheimer Research, 2014, 11, 367-388.	1.4	29
67	Real-time display of artifact-free electroencephalography during functional magnetic resonance imaging and magnetic resonance spectroscopy in an animal model of epilepsy. Magnetic Resonance in Medicine, 2005, 53, 456-464.	3.0	27
68	Association Between Ambulatory 24-Hour Blood Pressure Levels and Brain Volume Reduction. Hypertension, 2012, 60, 1324-1331.	2.7	27
69	Endothelin-1 induced MCAO: Dose dependency of cerebral blood flow. Journal of Neuroscience Methods, 2009, 179, 22-28.	2.5	26
70	ParaCEST MRI contrast agents capable of derivatizationvia "click―chemistry. Organic and Biomolecular Chemistry, 2012, 10, 287-292.	2.8	26
71	White matter integrity is associated with gait impairment and falls in mild cognitive impairment. Results from the gait and brain study. NeuroImage: Clinical, 2019, 24, 101975.	2.7	26
72	Changes in Functional Magnetic Resonance Imaging Cortical Activation After Decompression of Cervical Spondylosis. Neurosurgery, 2010, 67, E863-E864.	1.1	25

#	Article	IF	CITATIONS
73	Analogs of Eu3+ DOTAM-Gly-Phe-OH and Tm3+ DOTAM-Gly-Lys-OH: Synthesis and magnetic properties of potential PARACEST MRI contrast agents. Bioorganic and Medicinal Chemistry, 2008, 16, 6156-6166.	3.0	24
74	Cervical Spondylotic Myelopathy: Metabolite Changes in the Primary Motor Cortex after Surgery. Radiology, 2017, 282, 817-825.	7.3	24
75	Reduced brain glutamine in female varsity rugby athletes after concussion and in non oncussed athletes after a season of play. Human Brain Mapping, 2018, 39, 1489-1499.	3.6	24
76	Optimized in vivo brain glutamate measurement using longâ€echoâ€ŧime semi‣ASER at 7 T. NMR in Biomedicine, 2018, 31, e4002.	2.8	24
77	MR compatibility of EEG scalp electrodes at 4 tesla. Journal of Magnetic Resonance Imaging, 2007, 25, 872-877.	3.4	23
78	Clinical applications of neuroimaging in patients with Alzheimer's disease: a review from the Fourth Canadian Consensus Conference on the Diagnosis and Treatment of Dementia 2012. Alzheimer's Research and Therapy, 2013, 5, S3.	6.2	23
79	Vitamin D-related changes in intracranial volume in older adults: A quantitative neuroimaging study. Maturitas, 2015, 80, 312-317.	2.4	23
80	Ontario Neurodegenerative Disease Research Initiative (ONDRI): Structural MRI Methods and Outcome Measures. Frontiers in Neurology, 2020, 11, 847.	2.4	23
81	Comparison of quality control methods for automated diffusion tensor imaging analysis pipelines. PLoS ONE, 2019, 14, e0226715.	2.5	22
82	Sodium T2*-weighted MR imaging of acute focal cerebral ischemia in rabbits. Magnetic Resonance Imaging, 2004, 22, 983-991.	1.8	20
83	In vivo detection of PARACEST agents with relaxation correction. Magnetic Resonance in Medicine, 2010, 63, 1184-1192.	3.0	20
84	Vitamin D and Caudal Primary Motor Cortex: A Magnetic Resonance Spectroscopy Study. PLoS ONE, 2014, 9, e87314.	2.5	20
85	Motor network recovery in patients with chronic spinal cord compression: a longitudinal study following decompression surgery. Journal of Neurosurgery: Spine, 2018, 28, 379-388.	1.7	20
86	The Monocarboxylate transporter inhibitor Quercetin induces intracellular acidification in a mouse model of Glioblastoma Multiforme: in-vivo detection using magnetic resonance imaging. Investigational New Drugs, 2019, 37, 595-601.	2.6	20
87	Longitudinal changes of brain microstructure and function in nonconcussed female rugby players. Neurology, 2020, 95, e402-e412.	1.1	20
88	Registration of in vivo magnetic resonance T1-weighted brain images to triphenyltetrazolium chloride stained sections in small animals. Journal of Neuroscience Methods, 2006, 156, 368-375.	2.5	19
89	Water-soluble gold nanoparticles (AuNP) functionalized with a gadolinium(iii) chelate via Michael addition for use as a MRI contrast agent. Journal of Materials Chemistry B, 2013, 1, 5628.	5.8	19
90	Spontaneous low frequency BOLD signal variations from resting-state fMRI are decreased in Alzheimer disease. PLoS ONE, 2017, 12, e0178529.	2.5	19

#	Article	IF	CITATIONS
91	Ventricular volume expansion in presymptomatic genetic frontotemporal dementia. Neurology, 2019, 93, e1699-e1706.	1.1	19
92	Linked MRI signatures of the brain's acute and persistent response to concussion in female varsity rugby players. NeuroImage: Clinical, 2019, 21, 101627.	2.7	19
93	The effect of physical exercise on functional brain network connectivity in older adults with and without cognitive impairment. A systematic review. Mechanisms of Ageing and Development, 2021, 196, 111493.	4.6	19
94	Physiological monitoring of small animals during magnetic resonance imaging. Journal of Neuroscience Methods, 2005, 144, 207-213.	2.5	18
95	Metabolite and functional profile of patients with cervical spondylotic myelopathy. Journal of Neurosurgery: Spine, 2017, 26, 547-553.	1.7	18
96	Cortical Thickness Estimation in Individuals With Cerebral Small Vessel Disease, Focal Atrophy, and Chronic Stroke Lesions. Frontiers in Neuroscience, 2020, 14, 598868.	2.8	18
97	"Click―chemistry toward bis(DOTA-derived) heterometallic complexes: potential bimodal MRI/PET(SPECT) molecular imaging probes. RSC Advances, 2013, 3, 3249.	3.6	17
98	N-acetylaspartate in the motor and sensory cortices following functional recovery after surgery for cervical spondylotic myelopathy. Journal of Neurosurgery: Spine, 2016, 25, 436-443.	1.7	17
99	Brain tumor acidification using drugs simultaneously targeting multiple pH regulatory mechanisms. Journal of Neuro-Oncology, 2019, 144, 453-462.	2.9	17
100	Reproducibility of Neurite Orientation Dispersion and Density Imaging (NODDI) in rats at 9.4 Tesla. PLoS ONE, 2019, 14, e0215974.	2.5	17
101	Detection of Active Caspase-3 in Mouse Models of Stroke and Alzheimer's Disease with a Novel Dual Positron Emission Tomography/Fluorescent Tracer [⁶⁸ Ga]Ga-TC3-OGDOTA. Contrast Media and Molecular Imaging, 2019, 2019, 1-17.	0.8	17
102	Effects of overnight sleep restriction on brain chemistry and mood in women with unipolar depression and healthy controls. Journal of Psychiatry and Neuroscience, 2009, 34, 352-60.	2.4	17
103	Deep Bayesian networks for uncertainty estimation and adversarial resistance of white matter hyperintensity segmentation. Human Brain Mapping, 2022, 43, 2089-2108.	3.6	17
104	Quantitative short echo-time1H LASER-CSI in human brain at 4 T. NMR in Biomedicine, 2006, 19, 999-1009.	2.8	16
105	Highâ€field MRSI of the prostate using a transmit/receive endorectal coil and gradient modulated adiabatic localization. Journal of Magnetic Resonance Imaging, 2009, 30, 335-343.	3.4	16
106	Role of emerging neuroimaging modalities in patients with cognitive impairment: a review from the Canadian Consensus Conference on the Diagnosis and Treatment of Dementia 2012. Alzheimer's Research and Therapy, 2013, 5, S4.	6.2	16
107	A dual magnetic resonance imaging/fluorescent contrast agent for Cathepsinâ€Ð detection. Contrast Media and Molecular Imaging, 2013, 8, 127-139.	0.8	15
108	1H MR spectroscopy of the motor cortex immediately following transcranial direct current stimulation at 7 Tesla. PLoS ONE, 2018, 13, e0198053.	2.5	15

#	Article	IF	CITATIONS
109	In vivo detection of acute intracellular acidification in glioblastoma multiforme following a single dose of cariporide. International Journal of Clinical Oncology, 2018, 23, 812-819.	2.2	15
110	Neural effects of oxytocin and mimicry in frontotemporal dementia. Neurology, 2020, 95, e2635-e2647.	1.1	15
111	Characteristics of the Ontario Neurodegenerative Disease Research Initiative cohort. Alzheimer's and Dementia, 2023, 19, 226-243.	0.8	15
112	Transceive surface coil array for MRI of the human prostate at 4T. Magnetic Resonance in Medicine, 2007, 57, 455-458.	3.0	14
113	A DOTAMâ€based paraCEST agent favoring TSAP geometry for enhanced amide proton chemical shift dispersion and temperature sensitivity. Contrast Media and Molecular Imaging, 2013, 8, 289-292.	0.8	14
114	Association Between Serum 25â€Hydroxyvitamin D Concentration and Optic Chiasm Volume. Journal of the American Geriatrics Society, 2013, 61, 1026-1028.	2.6	14
115	Automated algorithm to measure changes in medial temporal lobe volume in Alzheimer disease. Journal of Neuroscience Methods, 2014, 227, 35-46.	2.5	14
116	The Dynamics of Impaired Blood-Brain Barrier Restoration in a Rat Model of Co-morbid Injury. Molecular Neurobiology, 2018, 55, 8071-8083.	4.0	14
117	Improved Segmentation of the Intracranial and Ventricular Volumes in Populations with Cerebrovascular Lesions and Atrophy Using 3D CNNs. Neuroinformatics, 2021, 19, 597-618.	2.8	14
118	Longitudinal Measurements of Intra- and Extracellular pH Gradient in a Rat Model of Glioma. Tomography, 2018, 4, 46-54.	1.8	14
119	Mono―and Tetraalkyne Modified Ligands and Their Eu ³⁺ Complexes – Utilizing "Click― Chemistry to Expand the Scope of Conjugation Chemistry. European Journal of Organic Chemistry, 2011, 2011, 6532-6543.	2.4	13
120	Association between muscle hydration measures acquired using bioelectrical impedance spectroscopy and magnetic resonance imaging in healthy and hemodialysis population. Physiological Reports, 2015, 3, e12219.	1.7	12
121	A new synthesis of cystamine modified Eu3+ DOTAM-Gly-Phe-OH: a conjugation ready temperature sensitive MRI contrast agent. Organic and Biomolecular Chemistry, 2008, 6, 3588.	2.8	11
122	A bifunctional chelator featuring the DOTAM-Gly-I-Phe-OH structural subunit: en route toward homo- and heterobimetallic lanthanide(III) complexes as PARACEST MRI contrast agents. Tetrahedron Letters, 2010, 51, 1087-1090.	1.4	11
123	A novel MRIâ€compatible brain ventricle phantom for validation of segmentation and volumetry methods. Journal of Magnetic Resonance Imaging, 2012, 36, 476-482.	3.4	11
124	Functional MRI of neuronal activation in epilepsy patients with malformations of cortical development. Epilepsy Research, 2015, 116, 1-7.	1.6	11
125	MRI-visible perivascular space volumes, sleep duration and daytime dysfunction in adults with cerebrovascular disease. Sleep Medicine, 2021, 83, 83-88.	1.6	11
126	Small and Large Magnetic Resonance Imaging–Visible Perivascular Spaces in the Basal Ganglia of Parkinson's Disease Patients. Movement Disorders, 2022, 37, 1304-1309.	3.9	11

#	Article	IF	CITATIONS
127	DOTAMâ€ŧype ligands possessing arginine pendant groups for use in PARACEST MRI. Contrast Media and Molecular Imaging, 2012, 7, 441-449.	0.8	10
128	MRI ParaCEST agents that improve amide based pH measurements by limiting inner sphere water T ₂ exchange. RSC Advances, 2014, 4, 1666-1674.	3.6	10
129	Prolonged In Vivo Retention of a Cathepsin D Targeted Optical Contrast Agent in a Mouse Model of Alzheimer's Disease. Journal of Alzheimer's Disease, 2015, 48, 73-87.	2.6	10
130	Memantine Plus Vitamin D Prevents Axonal Degeneration Caused by Lysed Blood. ACS Chemical Neuroscience, 2015, 6, 393-397.	3.5	10
131	The Canadian Dementia Imaging Protocol: Harmonization validity for morphometry measurements. NeuroImage: Clinical, 2019, 24, 101943.	2.7	10
132	Reduced power magnetic resonance spectroscopic imaging of the prostate at 4.0 Tesla. Magnetic Resonance in Medicine, 2009, 61, 273-281.	3.0	9
133	Synergistic toxicity in an in vivo model of neurodegeneration through the co-expression of human TDP-43M337V and tauT175D protein. Acta Neuropathologica Communications, 2019, 7, 170.	5.2	9
134	Structural Brain Magnetic Resonance Imaging to Rule Out Comorbid Pathology in the Assessment of Alzheimer's Disease Dementia: Findings from the Ontario Neurodegenerative Disease Research Initiative (ONDRI) Study and Clinical Trials Over the Past 10 Years. Journal of Alzheimer's Disease, 2020, 74, 747-757.	2.6	9
135	Concussion Acutely Decreases Plasma Glycerophospholipids in Adolescent Male Athletes. Journal of Neurotrauma, 2021, 38, 1608-1614.	3.4	9
136	Quantitative sodium MRI of the mouse prostate. Magnetic Resonance in Medicine, 2010, 63, 822-827.	3.0	8
137	Synthesis of MRI contrast agents derived from DOTAM-Gly-l-Phe-OH incorporating a disulfide bridge: Conjugation to a cell penetrating peptide and preparation of a dimeric agent. Bioorganic and Medicinal Chemistry Letters, 2010, 20, 5521-5526.	2.2	8
138	Multimodal neuroimaging of frontal white matter microstructure in early phase schizophrenia: the impact of early adolescent cannabis use. BMC Psychiatry, 2013, 13, 264.	2.6	8
139	Complexes of selected late period lanthanide(III) cations with 1,4,7,10-tetraazacyclododecane-1,4,7,10-tetraacetic acid amide (DOTAM)-alkyl ligands — A new platform for the development of paramagnetic chemical exchange saturation transfer (PARACEST) magnetic resonance imaging (MRI) contrast agents. Canadian lournal of Chemistry. 2013. 91. 211-219.	1.1	8
140	Use of Vitamin K Antagonists and Brain Volumetry in Older Adults: Preliminary Results From the <scp>GAIT</scp> Study. Journal of the American Geriatrics Society, 2015, 63, 2199-2202.	2.6	8
141	Characterization of clinical human prostate cancer lesions using 3.0â€T sodium MRI registered to Gleasonâ€graded wholeâ€mount histopathology. Journal of Magnetic Resonance Imaging, 2019, 49, 1409-1419.	3.4	8
142	Optimized MRI contrast for onâ€resonance proton exchange processes of PARACEST agents in biological systems. Magnetic Resonance in Medicine, 2009, 62, 1282-1291.	3.0	7
143	Nutrient Biomarker Patterns, Cognitive Function, and Mri Measures of Brain Aging. Neurology, 2012, 78, 1281-1282.	1.1	7
144	Unshielded asymmetric transmit-only and endorectal receive-only radiofrequency coil for ²³ Na MRI of the prostate at 3 tesla. Journal of Magnetic Resonance Imaging, 2015, 42, 436-445.	3.4	7

ROBERT BARTHA

#	Article	IF	CITATIONS
145	Introduction of Peripheral Carboxylates to Decrease the Charge on Tm ³⁺ DOTAM-Alkyl Complexes: Implications for Detection Sensitivity and in Vivo Toxicity of PARACEST MRI Contrast Agents. Journal of Medicinal Chemistry, 2015, 58, 6516-6532.	6.4	7
146	Illness versus substance use effects on the frontal white matter in early phase schizophrenia: A 4 Tesla 1 H-MRS study. Schizophrenia Research, 2016, 175, 4-11.	2.0	7
147	An Aspartyl Cathepsin Targeted PET Agent: Application in an Alzheimer's Disease Mouse Model. Journal of Alzheimer's Disease, 2018, 61, 1241-1252.	2.6	7
148	Semiautomated Assessment of the Anterior Cingulate Cortex in Alzheimer's Disease. Journal of Neuroimaging, 2019, 29, 376-382.	2.0	7
149	Multimodality In Vivo Imaging of Perfusion and Glycolysis in a Rat Model of C6 Glioma. Molecular Imaging and Biology, 2021, 23, 516-526.	2.6	7
150	Spinal cord compression is associated with brain plasticity in degenerative cervical myelopathy. Brain Communications, 2021, 3, fcab131.	3.3	7
151	Thalamic cramplike pain. Journal of the Neurological Sciences, 2014, 336, 269-272.	0.6	6
152	Effect of Memantine Treatment and Combination with Vitamin D Supplementation on Body Composition in the APP/PS1 Mouse Model of Alzheimer's Disease Following Chronic Vitamin D Deficiency. Journal of Alzheimer's Disease, 2021, 81, 375-388.	2.6	6
153	Neurite orientation dispersion and density imaging in a rodent model of acute mild traumatic brain injury. Journal of Neuroimaging, 2021, 31, 879-892.	2.0	6
154	4-T fMRI of the motor and sensory cortices in patients with polymicrogyria and epilepsy. Clinical Neurology and Neurosurgery, 2014, 122, 29-33.	1.4	5
155	Preliminary evaluation of PARACEST MRI agents for the detection of nitric oxide synthase. Canadian Journal of Chemistry, 2016, 94, 715-722.	1.1	5
156	Striatal Acetylcholine Helps to Preserve Functional Outcomes in a Mouse Model of Stroke. ASN Neuro, 2020, 12, 175909142096161.	2.7	5
157	Brain Metabolite Levels in Sedentary Women and Non-contact Athletes Differ From Contact Athletes. Frontiers in Human Neuroscience, 2020, 14, 593498.	2.0	5
158	Resting state fMRI scanner instabilities revealed by longitudinal phantom scans in a multi-center study. NeuroImage, 2021, 237, 118197.	4.2	5
159	Predicting Cognitive Impairment in Cerebrovascular Disease Using Spoken Discourse Production. Topics in Language Disorders, 2021, 41, 73-98.	1.0	5
160	Somatic Gene Transfer Using a Recombinant Adenoviral Vector (rAAV9) Encoding Pseudophosphorylated Human Thr175 Tau in Adult Rat Hippocampus Induces Tau Pathology. Journal of Neuropathology and Experimental Neurology, 2018, 77, 685-695.	1.7	4
161	Investigating the contribution of white matter hyperintensities and cortical thickness to empathy in neurodegenerative and cerebrovascular diseases. GeroScience, 2022, 44, 1575-1598.	4.6	4
162	Experimental validation of a T2ϕtransverse relaxation model using LASER and CPMG acquisitions. Journal of Magnetic Resonance, 2006, 181, 35-44.	2.1	3

#	Article	IF	CITATIONS
163	Efficient 3D rendering for web-based medical imaging software: a proof of concept. Proceedings of SPIE, 2011, , .	0.8	3
164	Reduced N-Acetylaspartate to Creatine Ratio in the Posterior Cingulate Correlates with Cognition in Alzheimer's Disease following Four Months of Rivastigmine Treatment. Dementia and Geriatric Cognitive Disorders, 2015, 39, 68-80.	1.5	3
165	Differential effects of transcranial direct current stimulation on antiphase and inphase motor tasks: A pilot study. Behavioural Brain Research, 2019, 366, 13-18.	2.2	3
166	Putative Concussion Biomarkers Identified in Adolescent Male Athletes Using Targeted Plasma Proteomics. Frontiers in Neurology, 2021, 12, 787480.	2.4	3
167	T2†measurement during acute cerebral ischemia by Carr-Purcell MRI at 4T. Magnetic Resonance in Medicine, 2005, 54, 1448-1454.	3.0	2
168	Enhanced diffusion weighting generated by selective adiabatic pulse trains. Journal of Magnetic Resonance, 2007, 188, 35-40.	2.1	2
169	Reliability of Calf Bioelectrical Impedance Spectroscopy and Magnetic-Resonance-Imaging-Acquired Skeletal Muscle Hydration Measures in Healthy People. Physiology Journal, 2013, 2013, 1-12.	0.4	2
170	Dysprosium(III) and thulium(III) complexes of DO3A-monoanilides: an investigation of electronic effects on their relaxometric and amide-based PARACEST properties. Canadian Journal of Chemistry, 2015, 93, 244-252.	1.1	2
171	Does the Neurological Examination Correlate with Patient-Perceived Outcomes inÂDegenerative Cervical Myelopathy?. World Neurosurgery, 2019, 132, e885-e890.	1.3	2
172	Magnetic Resonance Imaging Sequence Identification Using a Metadata Learning Approach. Frontiers in Neuroinformatics, 2021, 15, 622951.	2.5	2
173	Comparison of T2 and LASER T2†image contrast in a rat model of acute cerebral ischemia. Magnetic Resonance Imaging, 2008, 26, 323-329.	1.8	1
174	NPAS3 variants in schizophrenia: a neuroimaging study. BMC Medical Genetics, 2014, 15, 37.	2.1	1
175	P3â€379: BRAIN DIFFUSION TENSOR IMAGING METRICS IN ISCHEMIC LESIONS IN VASCULAR COGNITIVE IMPAIRMENT. Alzheimer's and Dementia, 2018, 14, P1238.	0.8	1
176	The Canadian Dementia Imaging Protocol: Harmonizing National Cohorts. Journal of Magnetic Resonance Imaging, 2019, 49, spcone.	3.4	1
177	Vitamin D concentration and lateral cerebral ventricle volume in older adults. , 2013, 57, 267.		1
178	Effects of Memantine and High Dose Vitamin D on Gait in Male APP/PS1 Alzheimer's Disease Mice Following Vitamin D Deprivation. Journal of Alzheimer's Disease, 2022, 85, 1755-1766.	2.6	1
179	Increased brain volumetric measurement precision from multi-site 3D T1-weighted 3ÂT magnetic resonance imaging by correcting geometric distortions. Magnetic Resonance Imaging, 2022, 92, 150-160.	1.8	1
180	Detection of small human cerebral cortical lesions with MRI under different levels of Gaussian smoothing: applications in epilepsy. Proceedings of SPIE, 2010, , .	0.8	0

#	Article	IF	CITATIONS
181	Metastatic brain cancer: prediction of response to whole-brain helical tomotherapy with simultaneous intralesional boost for metastatic disease using quantitative MR imaging features. , 2014, , .		0
182	P1â€273: Neuronal Activity Derived From Resting State Functional MRI: A Potential Biomarker for Alzheimer's Disease. Alzheimer's and Dementia, 2016, 12, P521.	0.8	0
183	ICâ€Pâ€121: Neuronal Activity Derived from Resting State Functional MRI: A Potential Biomarker for Alzheimer Disease. Alzheimer's and Dementia, 2016, 12, P90.	0.8	Ο
184	A preliminary magnetic resonance spectroscopy study of postmenopausal hormone effects on the brain. Minerva Ginecologica, 2019, 71, 392-393.	0.8	0
185	Brain pH Measurement Using AACID CEST MRI Incorporating the 2 ppm Amine Resonance. Tomography, 2022, 8, 730-739.	1.8	0